JOURNAL OF THERMOPHYSICS AND HEAT TRANSFER
Vol. 11, No. 2, April–June 1997

Post-Critical Heat Flux Swirl Flow Heat Transfer with Two Refrigerants and Water

S.-J. Yoo,* D. M. France,† and T. M. Tarshish‡
University of Illinois at Chicago, Chicago, Illinois 60607-7022

Boiling heat transfer in the post-critical heat flux (post-CHF) regime was studied experimentally under steady-state swirl flow conditions with low superheat temperatures of the heated surface. Experiments were performed with the vertical flow of refrigerant-113 (R-113) in a tube with an i.d. 7.75 mm and with a heated length of 3.66 m over the mass flux range of 375–535 kg/m^2 s at a pressure of 0.184 MPa. The use of R-113 as the boiling fluid significantly extended the property ranges of available post-CHF swirl-flow data. The swirl flow was generated in the refrigerant tube by the use of four twisted metal tapes with tape-twist ratios ranging from 2.5 to 9.2. Liquid heating produced the low-wall superheat (below 50°C) in the post-CHF region, that was stable at steady state, and that was typical of the operation of many heat exchangers. Superheated vapor measured at the test section exit in most tests ensured that the entire post-CHF region was included. R-113 data were compared with data for water and refrigerant-12. A form of an existing correlation for post-CHF swirl flow heat transfer was generalized, resulting in good predictions of both magnitudes and trends of the data of all three fluids.

Nomenclature

a = radial acceleration, m/s^2
C_h = correlating parameter in Eq. (5), (W s^4/m^6 K)$^{0.4}$
c_p = specific heat, J/kg K
D = diameter, m
D_H = hydraulic diameter, m
F = drop-wall interaction factor, m$^{-1/4}$
f = fin effect parameter of Eq. (6)
G = mass flux, kg/m^2 s
g = acceleration of gravity, m/s^2
h = heat transfer coefficient, kW/m^2 K
i_{lv} = latent heat of vaporization, J/kg
k = thermal conductivity, kW/m K
m = mass flow rate, kg/s
P = pressure, kPa
Pc = thermodynamic critical pressure, kPa
Pr = Prandtl number
q'' = heat flux at tube inner surface, kW/m^2
$Re_{v,a}$ = Reynolds number for axial vapor flow, $(\rho V_a D_H/\mu)_v$
$Re_{v,s}$ = Reynolds number for swirl vapor flow, $(\rho V_s D_H/\mu)_v$
T = temperature, °C
V = velocity, m/s
X = quality
Y = tape-twist ratio, length of 180 deg of twist/D_i
z = axial distance in direction of refrigerant flow, m
β = coefficient of volumetric thermal expansion, °C^{-1}
ΔT_{sat} = $T_{wi} - T_{sat}$, °C
μ = dynamic viscosity, kg/m s
ρ = density, kg/m^3
ψ = fraction of tube surface area for wall to drop heat transfer

Subscripts
a = axial
CHF = critical heat flux
h = heating fluid
i = tube inner surface
l = liquid
l-w = wall to drop
o = tube outer surface
R-113 = bulk condition of R-113
s = shell inner surface
sat = saturated
v = vapor
v,a = vapor axial flow
v,s = vapor swirl flow
v-w = wall to vapor
w = tube wall
wi = inner tube wall surface
wo = outer tube wall surface

Received June 11, 1996; revision received Nov. 26, 1996; accepted for publication Nov. 27, 1996.

*Currently Assistant Professor, Yong-In Technical College, Republic of Korea.
†Professor, Department of Mechanical Engineering.
‡National Science Foundation Graduate Fellow, Department of Mechanical Engineering.

Introduction

MANY types of heat transfer augmentation devices have been studied by numerous investigators for application to both single- and two-phase flows. Reviews of the literature are available.[1,2] An analysis of heat transfer enhancing mechanisms associated with various types of devices[3] showed that devices that produce a swirl component in single-phase flows are very efficient in increasing heat transfer rates. These devices also can be successful in increasing heat transfer rates in two-phase flows. One such swirl-inducing device is the twisted-tape insert for tube flows. Twisted-tapes have been shown to increase heat transfer rates in all modes of heat transfer and to be very efficient in delaying, to a higher quality, the critical heat flux (CHF) condition in two-phase flows. Important two-phase applications of such devices are in refrigeration and air-conditioning evaporators where there can be substantial size reduction benefits. Twisted-tape inserts in tubes are attractive for retrofit situations.

Most of the experimental investigations into enhanced heat transfer by means of twisted-tape inserts have been performed in single-phase flows; studies into two-phase forced convection heat transfer are sparse by comparison. The post-critical heat flux (post-CHF) region in particular has received little attention until recently. This region, characterized as a continuous vapor phase with discrete entrained liquid drops, is typically the least-efficient two-phase heat transfer regime. Many heat exchangers that operate with a post-CHF region can potentially

benefit from the heat transfer enhancement afforded by an induced swirl flow.

Mechanisms

The post-CHF two-phase-flow regime is also referred to as the liquid-deficient regime or as mist flow, and the majority of previous two-phase flow heat transfer investigations in this regime have been performed for axial flow conditions. In axial two-phase flow, post-CHF heat transfer has been modeled and correlated based on physical phenomena by many investigators. Three mechanisms are often recognized, heat transfer: 1) from the wall to the vapor, 2) from the vapor to the drops, and 3) directly from the wall to the drops.[4–7] The large majority of post-CHF heat transfer data in the engineering literature (including axial and swirl flows) were obtained under the condition of high-wall superheat, whereas low-wall superheat is indicative of many heat exchangers. These high-wall superheat studies have indicated that the heat transfer contribution from the direct interaction of the drops with the heated tube wall is small. However, recent low-wall superheat data[8,9] indicate an increase in importance in this heat transfer mechanism. Whether or not the drops wet the wall, direct drop-wall heat transfer becomes more important as wall superheat decreases.

Pioneering work[10] in the area of swirl flow heat transfer in the post-CHF regime considered the effect of the azimuthal velocity component on wall-to-vapor heat transfer rate. In addition, it accounted for the body force-induced flow resulting from the radial acceleration, produced by the twisted tape, in the direction of the heated wall. The database, used for developing a heat transfer correlation equation,[10] came from experiments with nitrogen at cryogenic temperatures, at very low mass fluxes in the range of 30–140 kg/m^2 s, and at moderate- to high-wall superheats of 60–300°C. Later, post-CHF swirl flow experiments were performed with water[8] and refrigerant-12[9] (R-12) over a larger mass flux range and at low-wall superheats. Heat transfer correlation equations were developed separately for each fluid, accounting for these same mechanisms.

Objective

The objective of this study was to experimentally investigate heat transfer in swirling two-phase flow in the post-CHF region generated by twisted-tape inserts in the flow. Refrigerant-113 (R-113) was chosen as the boiling fluid because its thermal properties are significantly different from the available data for water and R-12. Experiments were performed at steady state and low-wall superheat, both of which are typical of the operating conditions of many heat exchangers. An important objective was to develop a correlation equation capable of predicting post-CHF swirl flow heat transfer for the entire data range of the three fluids: 1) R-113, 2) R-12, and 3) water.

Experimental Approach

Flow Boiling Facility

Experiments were performed in the Flow Boiling Facility (FBF) in the Boiling Heat Transfer Laboratory at the University of Illinois at Chicago. The facility was developed to obtain more understanding of two-phase flow heat transfer phenomena, especially in the post-CHF region by providing for steady-state testing in that region. This steady-state condition is in contrast to most post-CHF heat transfer experimental data that were obtained using special techniques such as hot patches or transients to overcome the problem of an inherently unstable post-CHF region when a constant heat flux is imposed at the tube wall. However, many heat exchangers operate with a steady-state post-CHF region as a result of fluid heating. The FBF was designed specifically to produce such heat-exchanger conditions. This approach requires a relatively long test section because of the low-temperature differences between the tube wall and boiling fluid, and it requires more elaborate data acquisition/reduction techniques compared to the commonly used method of electrical resistance heating of the tube wall.

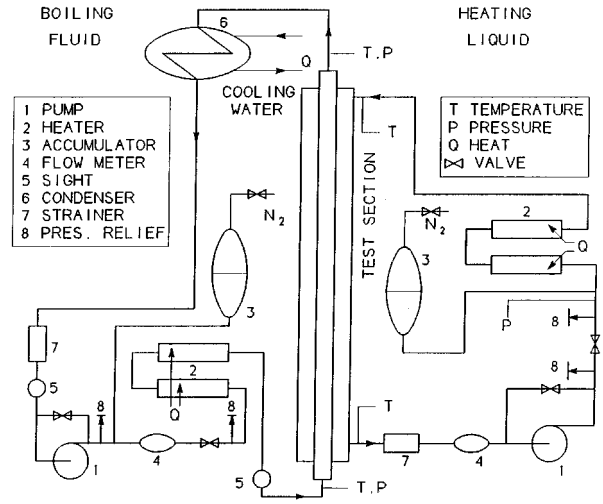

Fig. 1 Flow boiling facility.

The FBF is shown schematically in Fig. 1. Closed-pumped fluid circuits are shown for the boiling fluid (R-113) and the heating fluid (water). During the experiments, heat was supplied to the water by a series of eight electric cartridge heaters in the flow circuit which, with variac control, covered the range of 0–12 kW. The water circuit was designed to operate at a maximum pressure of 2760 kPa at a maximum temperature of 177°C. Hot water flowed from the heaters to the top of the facility from which it entered the test section flowing downward and exiting at the pump suction. The pumps in both the water and R-113 systems were of the positive displacement type with magnetically coupled motor drives, which eliminated pump shaft seals. They produced a flow rate of 0.2 l/s with a head of 140 kPa and were capable of operation at maximum system pressure of 2760 kPa. Pressure was controlled in each fluid system by accumulators using compressed nitrogen or air as the pressure supply.

As shown in Fig. 1, the boiling fluid R-113 was pumped as a liquid through preheaters to the bottom of the test section from which it flowed upward inside the test section tube containing a twisted-tape insert. The refrigerant boiled as it flowed through the test section, exiting to a water-cooled condenser (water temperature = 12°C), either as superheated vapor or in the quality range. The accumulator maintained prescribed system pressure in conjunction with the condenser operation. After the condenser, subcooled R-113 passed through a strainer and sight glass before returning to the pump.

Facility instruments included turbine flow meters in each fluid system. These instruments had an accuracy of better than 2% of the reading, and the electrical outputs were fed to a computer-controlled data acquisition system (DAS). Boiling circuit pressure was measured at the test section inlet, and a differential pressure was measured across the test section. Both measurements used capacitance-type electronic pressure transducers that were calibrated to an absolute accuracy of ±0.7 kPa, and outputs were fed to the DAS.

All instrument outputs, temperature, pressure, and flow from the FBF and test section were read by the DAS, which consisted of a computer-controlled Hewlett Packard (HP) 3497A test and measurement unit with 80 input channels. The HP 3497A voltmeter read $5\frac{1}{2}$ digits and was used in the 1-μV resolution range with common mode and ground loop electronic noise rejection. Under these conditions, information was brought to the DAS at the rate of 30 samples/s, which allowed the shell thermocouples (described subsequently) to be read in less than 2 s. This speed was sufficient to provide essentially an instantaneous recording of the shell temperatures uninflu-

enced by transition boiling and CHF movements in the test section that had a period of the order of 1 min. During data acquisition, the DAS was programmed to record the 57 shell thermocouple outputs and 10 reading averages from the pressure transducers and flow meters. Transducer averaging minimized electronic noise effects. During test set up, the instrument outputs were read by the DAS, changed to engineering units, and displayed on the DAS monitor. These readings were continuously updated to aid in reaching the prescribed parameters for each test.

Test Section

A schematic diagram of the FBF test section used in this study is given in Fig. 2. The test section was a counterflow, concentric-tube heat exchanger with a vertical heated length of 3.66 m. The boiling refrigerant flowed upward in the tube with a twisted-tape insert while the heating fluid flowed downward in the surrounding annulus. The refrigerant tube was made of copper with an i.d. of 7.75 mm and a wall thickness of 0.885 mm. The surrounding annulus tube (shell) had an i.d. of 16.56 mm. At the bottom of the test section, there was a 0.9-m-long tube assembly that had two sliding O-ring seals where the refrigerant tube and shell could slide with respect to one another to accommodate differential thermal expansion. The shell and tube of the test section were maintained in a concentric position by using five spacers located 0.61 m apart axially, and shell temperature measurements were made by 57 Cr–Al thermocouples spot welded along its length. The axial thermocouple spacing varied from 0.1524 to 0.0381 m near the refrigerant outlet to the test section. Nonuniform thermocouple spacing was employed to increase the accuracy of the measured temperature profile in the region of CHF where the largest axial thermal gradients occurred in the test section. Shell thermocouple outputs were read by the DAS as were outputs from sheathed thermocouples located in the streams of the two fluids as they entered and exited the test section. The entire test section was insulated with fiberglass to a thickness of 51 mm.

Twisted-tapes used in the tube flow were fabricated by cold-processing thin brass ribbon stock. The width of the tapes was 7.5 mm with a thickness of 0.5 mm, which provided a loose enough fit to allow the tapes to be pulled through the tube, yet tight enough to prevent bypass flow past the tape. The degree of the helical twist of a tape is usually designated by a dimensionless tape-twist ratio, Y = (length of 180 deg of tape-twist)/(tube i.d.).

Test Procedures

Isothermal tests served as an in-place calibration of the shell thermocouples using as standards the in-stream sheathed thermocouples that were externally calibrated against National Institute of Standards and Technology (NIST) traceable precision

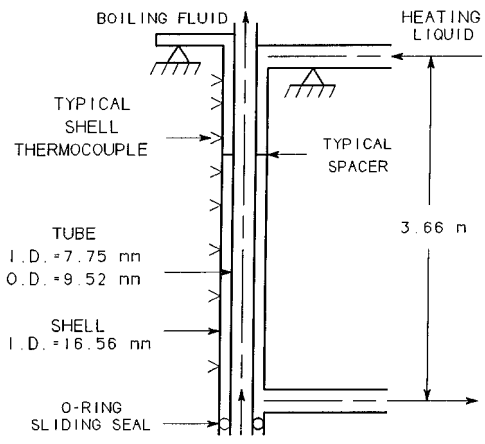

Fig. 2 Test section.

thermometers with an accuracy of ±0.05°C. An isothermal test was run at the maximum water flow rate with the R-113 side of the test section evacuated. Thermocouple temperatures were read multiple times and averaged by the DAS. Comparing the shell temperatures with the stream temperatures produced an end-to-end calibration of the shell thermocouples with an accuracy of ±0.2°C. Heat loss from the test section was determined experimentally in a similar manner to the isothermal tests, except the water flow rate was at a minimum. The heat loss from the shell to the atmosphere was determined to be very small, but it was included in the data reduction calculations.

Overall system performance was checked by heat balance tests where the test section was operated as a liquid–liquid counterflow heat exchanger. Heat balances calculated from the liquid tests were with the range of ±5%, and they were often below 2% in the boiling tests with outlet superheat.

For later use in data reduction and correlation, it was necessary to determine accurate correlations over the parameter ranges of interest for both the single-phase tube and annulus heat transfer coefficients. To this end, a series of tests was performed using a modified[11] Wilson plot technique.[12] Starting with the original technique, a series of tests was performed varying the annulus flow rate while holding the tube flow rate and Prandtl number constant. The assumption was made that the annulus heat transfer coefficient was proportional to the annulus Reynold's number raised to a power. In the modified technique, a similar set of tests was run where the tube flow rate was varied while the annulus side was fixed. The results from these two test series determined optimum exponents for the annulus and tube Reynolds numbers. The results were that the Monrad[13] correlation for the heat transfer coefficient of water flowing in an annulus predicted the data well as found previously[9,11,14]; it is given by

$$h_h(D_s - D_o)/k_h = 0.02Re_h^{0.8}Pr_h^{1/3}(D_s/D_o)^{0.53} \qquad (1)$$

A slight improvement in the predictions of Eq. (1) was obtained by increasing the Reynolds number exponent slightly, but the data reduction was not sensitive to the change.

The modified Wilson plot technique[12] also produced a tube heat transfer correlation of the Dittus and Boelter type,[15] which was used in subsequent data correlation efforts. The data were predicted well by the Gnielinski correlation,[16] but overpredicted somewhat by the Dittus and Boelter equation.[15] In compensation, the leading constant in the Dittus and Boelter correlation[15] was reduced for later use in correlation of two-phase data.

Subsequent to the single-phase tests described, two-phase testing was performed in the FBF. The parameters that specified a boiling test were the flow rates and the inlet temperatures of each fluid, the R-113 pressure, and the location of CHF or the exit R-113 superheat. Most tests were conducted with a measurable exit superheat to ensure that the entire post-CHF region was present in the test section. A total of 95 tests was performed over an R-113 mass flux range of 375–535 kg/m^2 s, using four twisted-tapes with Y = 2.5, 4.2, 6.25, and 9.2. The refrigerant pressure was approximately constant throughout the tests at 184 kPa absolute. In each test, the DAS was used initially in the setup mode where system and test section parameters were continuously monitored until steady state was reached at the desired parameters. The DAS was then changed to the data acquisition mode where instrument readings were recorded to computer disk for later analysis.

Data Reduction

Axial parameter distributions from a typical boiling test are shown in Fig. 3. The open symbols represent the shell thermocouples, and the axial distance z is measured in the direction of the boiling refrigerant flow. The first step in the data reduction procedure was to smooth the shell temperature measurement using cubic splines that were not forced through the

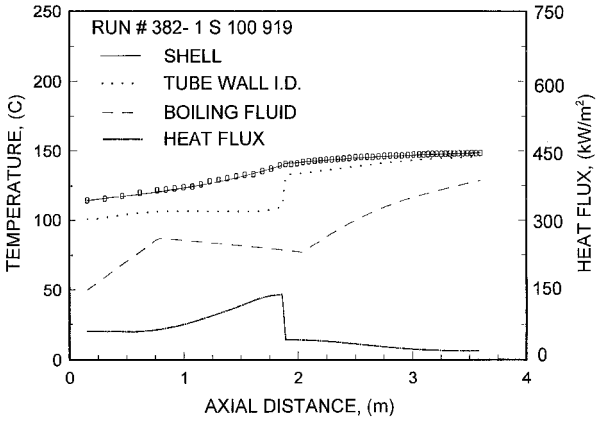

Fig. 3 Typical axial distributions.

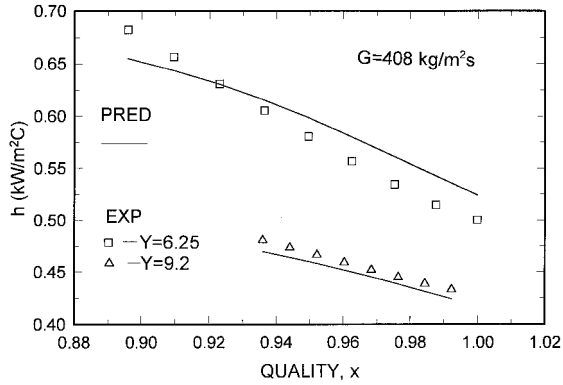

Fig. 4 Local post-CHF results.

measured points. The solid line through the open symbols in Fig. 3 is the result of such a spline calculation. It has been shown[17] that the water flow for this type of system is essentially fully developed thermally; consequently, the heat flux to the boiling fluid was calculated from the gradient of the shell temperatures as

$$q''(z) = \frac{(mc_p)_h}{\pi D_i}\frac{\mathrm{d}T_s(z)}{\mathrm{d}z} \tag{2}$$

Then the wall temperature of the tube outside surface T_{wo} was calculated from

$$T_{wo}(z) = T_s(z) - [q''(z)D_i/h_hD_o] \tag{3}$$

where the annulus heat transfer coefficient h_h was calculated from the Monrad relation, Eq. (1). The inside surface temperature of the boiling tube T_{wi} was calculated from a cylindrical coordinate conduction equation as

$$T_{wi}(z) = \frac{q''(z)(D_i/2)\ell n(D_o/D_i)}{k_w} + T_{wo}(z) \tag{4}$$

where q'' is positive in the outward radial direction.

Following the calculation of the axial heat flux distribution, the boiling fluid enthalpy was found from a heat balance. Using the local enthalpy and the pressure (determined from the system and differential measurements), the boiling fluid temperature and equilibrium quality were determined as a function of axial distance as well. The heat flux, tube inside surface temperature, and R-113 temperatures are shown in Fig. 3 as a function of z. The peak in the heat flux occurring at $z = 1.85$ m is the CHF point, and it corresponds to a sharp increase in tube wall temperature. The post-CHF region is between the minimum in the heat flux curve and the point where the quality is equal to unity that occurs, under equilibrium conditions, where the boiling fluid temperature begins to rise in the superheat region in Fig. 3 at $z = 2.1$ m. In the test of Fig. 3, the wall superheat in the post-CHF region is approximately 50°C. This level of superheat is low enough to represent heat exchanger operation, yet high enough to produce good accuracy in the R-113 heat transfer coefficient defined in the usual way as $h = q''/(T_{wi} - T_{R\text{-}113})$. (Uncertainty of ±0.25°C in these two temperatures results in a small uncertainty in h of 1% at this wall superheat of 50°C.)

Results and Discussion

The R-113 heat transfer data followed the general trends of previous investigations with other boiling fluids, however, magnitudes were significantly different. The swirl component of the flow induced by the twisted-tapes increases the heat transfer coefficient in the post-CHF region compared to the axial-flow (open-tube) case. The tapes also increase the quality at the CHF point; both phenomena provide heat transfer enhancement. Typical local heat transfer coefficient results, along the post-CHF region in the test section, are shown in Fig. 4 from two tests at the same refrigerant mass flux, $G = 408$ kg/m^2 s and different tape-twist ratios. The effect of higher accelerations as a result of tighter tape-twists (lower values of Y) is to increase the heat transfer coefficients as seen in Fig. 4 for the present tests with R-113. The predictions shown in Fig. 4 were calculated from a correlation equation (discussed next) that was developed using these data and data from the swirl flow of water and R-12.

Data Prediction

In earlier developments of separate correlation equations for post-CHF heat transfer to the swirl flow of water[8] and R-12[9] at low-wall superheat, it was found that the formulation of Bergles et al.[10] provided a good foundation. That formulation included the mechanisms of heat transfer from the heated wall to the vapor, from the heated wall to the drops, and the influence of the body force-induced flow. The twisted-tape-induced mixing of drops and vapor coupled with low-wall superheat conditions support the thermodynamic equilibrium approach of the formulation that implicitly accounts for heat transfer between vapor and drops. In the R-12 work,[9] the effect of the boiling number was found to improve the correlation of the data. That work was followed in developing an equation based on physical parameters for predicting the heat transfer coefficient for three fluids (R-113, water, and R-12) that covered the large data parameter range given in Table 1.

The swirl flow post-CHF heat transfer equation developed[9] for R-12, and based on earlier work with nitrogen[10] and water,[8] has the form

$$h = C_h[\psi h_{l\text{-}w} + (1 - \psi)h_{v\text{-}w}]^{a'}\left[\frac{(T_w - T_{sat})}{G}\, i_{lv}\right]^{b'} \tag{5}$$

where C_h, a', and b' are constants that were optimized for R-12. The heat transfer coefficient between the tube wall and the vapor flow was taken[18] from single-phase swirl flow investigations at low-wall superheat as in the present experiments:

$$(1 - \psi)Nu_{v\text{-}w} = f\left\{c' Re_{v,s}^{0.8} Pr_v^{0.4} + d'\left[\left(\frac{Re_{v,a}}{Y}\right)^2\left(\frac{D_H}{D_i}\right)\beta_v(T_w - T_{sat})Pr_v\right]^{1/3}\right\} \tag{6}$$

The first term inside the braces of Eq. (6) represents forced convection heat transfer between the wall and the swirling vapor flow with the coefficient c', and the second term represents the body force-induced flow with coefficient d'. $Re_{v,s}$ is based

Table 1 Post-CHF Swirl Flow Data Ranges

Fluid	G, kg/m^2 s	ΔT_{sat}, °C (maximum)	P/Pc	Y	ρ_l/ρ_v	Number of tests
Water	910–1878	40	0.7	2.55–7.5	5.5	21
R-12	140–1300	60	0.25	2.5–9.2	20	80
R-113	375–535	50	0.054	2.5–9.2	99	95

on the resultant swirl velocity V_s, which is related to the axial component of velocity V_a as follows:

$$V_s = (V_a/2Y)(4Y^2 + \pi^2)^{0.5} \tag{7}$$

$$V_a = (G/\rho_l)[1 + X[(\rho_l/\rho_v) - 1]] \tag{8}$$

The hydraulic diameter in $Re_{v,s}$ and $Re_{v,a}$ in Eq. (6) is for the refrigerant tube with a twisted-tape insert, and the parameter f in Eq. (6) represents the fin effect of the twisted-tape from the tube wall. This effect was small in the present study because of the small contact area between the tapes and the tube surface. Thus, f was taken as unity.

Heat transfer between the tube wall and liquid drops is a function of the radial acceleration imparted to the flow by the twisted-tapes. It was modeled[19] from experiments with drops on heated surfaces with the addition of a drop acceleration effect $F(a/g)$:

$$\psi h_{l\text{-}w} = 1.1\left[\frac{k_v^3 i_{lv}^* a \rho_l \rho_v}{(T_w - T_{sat})\mu_v(\pi/6)^{1/3}}\right]^{1/4} \times \left\{\frac{(1-X)6/\pi}{X[(\rho_l/\rho_v) - 1] + 1}\right\}^{2/3} \frac{\pi}{4} F\left(\frac{a}{g}\right) \tag{9}$$

a is given by

$$a = (V_a\pi)^2/2D_iY^2 \tag{10}$$

and i_{lv}^* is a modified latent heat of evaporation given by

$$i_{lv}^* = i_{lv}\left[1.0 + \frac{7}{20}\frac{c_{p,v}(T_w - T_{sat})}{i_{lv}}\right]^{-3} \tag{11}$$

Equations (5), (6), and (9) specify the post-CHF swirl flow heat transfer coefficient, and the results of previous studies were to produce different values for the constants C_l, a', b', c', d', and the parameter $F(a/g)$ for water and R-12. The three-fluid database, formed with the addition of the present experiments using R-113, exhibited large variations in fluid properties and radial acceleration. The R-113 experiments exhibited the largest accelerations because of the very high ratio of liquid to vapor density as shown in the typical comparison of Fig. 5 for the mass flux ranges of the data at an approximately constant tape-twist ratio. Using data from the three fluids, the constants were optimized as $a' = 1.0$, $b' = 0.4$, $c' = 0.0195$, and $d' = 0.083$. The acceleration factor was previously found to be a function of acceleration and quality for a single fluid. In extending the results to three fluids, the density ratio of liquid to vapor was added to account for boiling fluid properties, and the factor F became

$$F = C_1 \exp\left[4.425 - C_2\left(\frac{a}{g}\right)^{1.1}\right](a/g)^{1.1}\left[\frac{2(1-X)}{(1+X_{CHF})}\right]^{0.5} \tag{12}$$

where parameters C_1 (m$^{-1/4}$) and C_2 (dimensionless) are

$$C_1 = 0.0095 - 7.9 \times 10^{-5}(\rho_l/\rho_v) \tag{13}$$

$$C_2 = [-8.59 + 3.49(\rho_l/\rho_v)] \times 10^{-6} \tag{14}$$

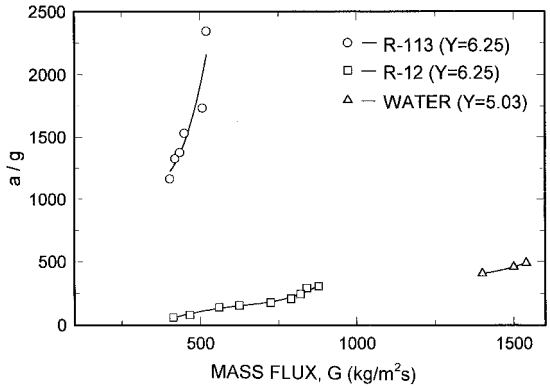

Fig. 5 Radial accelerations of three fluids.

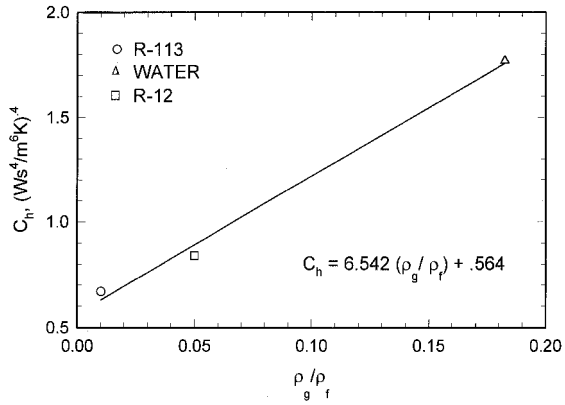

Fig. 6 Evaluation of heat transfer coefficient parameter C_h.

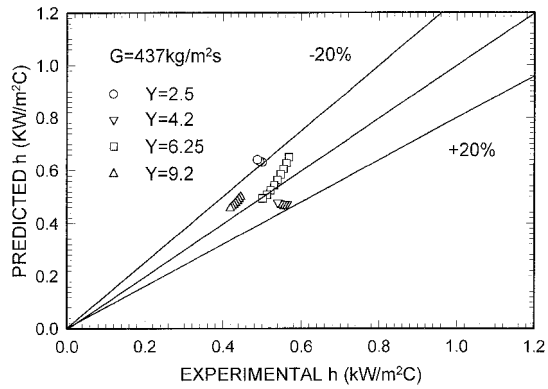

Fig. 7 Prediction of R-113 data at specific tape twist ratios.

The fluid acceleration incorporated into Eq. (12) effectively models the increased influence of drop-wall interaction at high accelerations. At low accelerations, F is limited to a value of 7.0, as found previously.[10] Finally, the parameter C_h was also found to be a function of fluid density ratio as

$$C_h = 6.542(\rho_g/\rho_l) + 0.564 \tag{15}$$

and the comparison of Eq. (15) with C_h results for individual fluids tested is shown in Fig. 6.

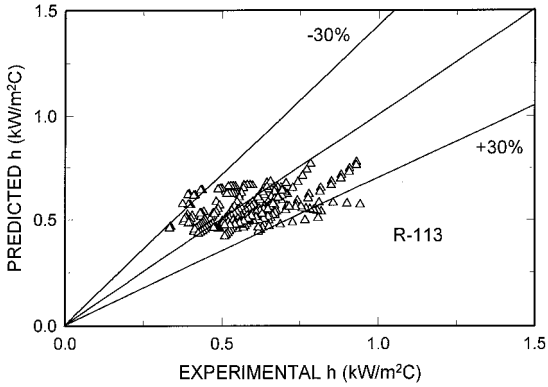

Fig. 8 Prediction of all R-113 data.

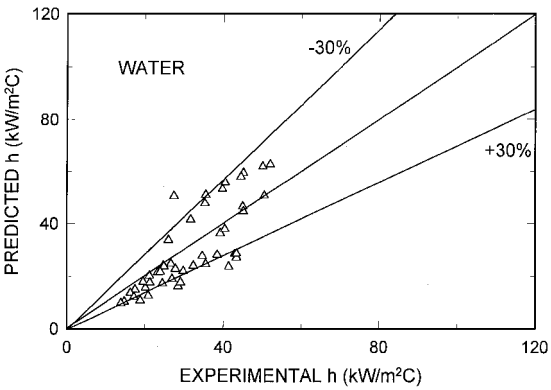

Fig. 9 Prediction of high-pressure water data.

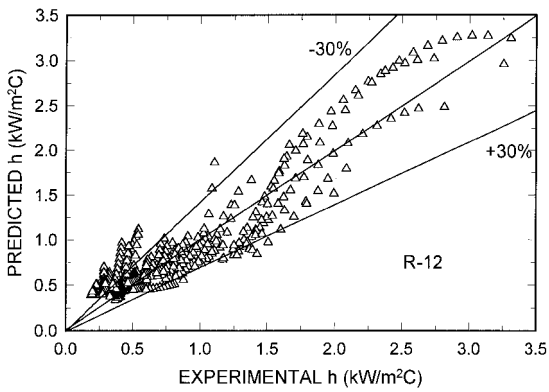

Fig. 10 Prediction of R-12 data.

Comparisons of Data and Predictions

The heat transfer coefficient predictions from Eqs. (5), (6), and (9) are compared to experimental results for post-CHF swirl flow of R-113 in Figs. 4 and 7. In each figure, the data are for a single representative mass flux and different tape-twist ratios. No systematic error is observed with Y, and the predictions are considered to be in good agreement with the experimental results. A further comparison with all of the R-113 data is shown in Fig. 8 where all of the data at all mass fluxes and all four tape-twist ratios of the study are plotted.

Similar comparisons to Fig. 8 are given in Figs. 9 and 10 for water and R-12, respectively. A composite of all data for the three fluids is given in Fig. 11, where again, comparison with prediction is considered to be good, and the error bands of ±30% as given in Figs. 8–10 also apply to Fig. 11.

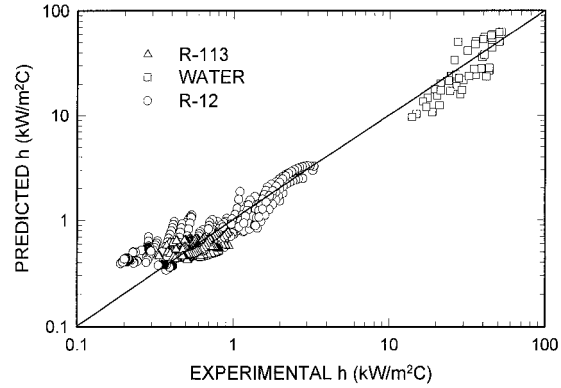

Fig. 11 Prediction of all data from three fluids.

Conclusions

The effect of twisted-tape-induced swirl flow on heat transfer in the post-CHF region was studied experimentally using R-113 under the condition of low-wall superheat. Liquid heating of the boiling refrigerant was used to obtain measurements under steady-state conditions indicative of operation of many two-phase heat exchanger evaporators. At operating pressure, the high-density ratio of the R-113 produced high radial accelerations with the twisted-tapes, which served to expand the existing database. The variation in fluid properties of the R-113 from available data in high-pressure water and R-12 also was significant in expanding the database. Ninety-five experiments were performed with R-113 using four twisted-tapes, and in each test heat transfer coefficients were determined in the entire post-CHF region up to a quality of unity.

Because of the very high radial fluid acceleration in the R-113 experiments compared to previous studies, existing correlation equations for predicting the heat transfer were considerably outside their database ranges and proved to be inaccurate. The effect of these high accelerations on post-CHF swirl flow heat transfer were attributed to the wall-drop contribution.

Accounting for a large range of fluid accelerations and fluid properties, a single heat equation was developed for the heat transfer coefficient in post-CHF swirl flow under conditions of low-wall superheat. This equation is based on experimental data from the current study with R-113 as well as available data with water and R-12 as the boiling fluids. The total parameter ranges for all fluids are $140 \leq G \leq 1878$ kg/m^2 s, $2.5 \leq Y \leq 9.2$, $5.5 \leq \rho_l/\rho_g \leq 99$, and wall superheat ≤ 60°C.

References

[1]Webb, R. L., *Principles of Enhanced Heat Transfer*, Wiley, New York, 1994.

[2]Bergles, A. E., Nirmalan, V., Junkham, G. H., and Webb, R. L., *Bibliography on Augmentation of Convective Heat and Mass Transfer-II*, Iowa State Univ., HTL-31, ISU-ERI-Ames-84221, Ames, IA, 1983.

[3]Rabas, T. J., "Selection of the Energy-Efficient Enhancement Geometry for Single-Phase Turbulent Flow Inside Tubes," *Heat Transfer Equipment Fundamentals, Design, Applications and Operation Problems*, American Society of Mechanical Engineers, HTD-Vol. 108, New York, 1989, pp. 193–204.

[4]Groeneveld, D. C., "Post-Dryout Heat Transfer at Reactor Operating Conditions," *Atomic Energy of Canada Limited Report*, 4513, Chalk River, ON, Canada, 1973.

[5]Plummer, D. N., Griffith, P., and Rohsenow, W. M., "Post-Critical Heat Transfer to Flowing Liquid in a Vertical Tube," *Transactions of the Canadian Society of Mechanical Engineering*, Vol. 4, 1976, pp. 151–158.

[6]Varone, A. F., and Rohsenow, W. M., "Post-Dryout Heat Transfer in Steam Generator Tubes at High Pressures," *International Journal of Heat and Mass Transfer*, Vol. 26, 1986, pp. 315–327.

[7]Koizumi, Y., Ueda, T., and Tanaka, T., "Post-Dryout Heat Transfer to R-113 Upward Flow in a Vertical Tube," *International Journal of Heat and Mass Transfer*, Vol. 22, 1979, pp. 669–678.

[8]Papadopoulos, P., France, D. M., and Minkowycz, W. J., "Heat Transfer to Dispersed Swirl Flow of High Pressure Water with Low Wall-Superheat," *Experimental Heat Transfer*, Vol. 4, 1991, pp. 153–169.

[9]Papadopoulos, P., France, D. M., Minkowycz, W. J., Harty, J., Hamoudeh, M. N., and Wu, M.-S., "Two-Phase Dispersed Flow Heat Transfer Augmented by Twisted Tapes," *Enhanced Heat Transfer*, Vol. 1, No. 4, 1994, pp. 305–314.

[10]Bergles, A. E., Fuller, W. D., and Hynek, S. J., "Dispersed Flow Film Boiling of Nitrogen with Swirl Flow," *International Journal of Heat and Mass Transfer*, Vol. 14, 1971, pp. 1343–1354.

[11]Panchal, C. B., and France, D. M., "Heat Transfer and Pressure Drop in Large Pitch Spirally Indented Tubes," *International Journal of Heat and Mass Transfer*, Vol. 36, 1993, pp. 565–576.

[12]Wilson, E. E., "A Basis for Rational Design of Heat Transfer Apparatus," *Transactions of the American Society of Mechanical Engineers*, Vol. 37, 1915, pp. 47–82.

[13]Monrad, C. C., and Pelton, J. F., "Heat Transfer by Convection in Annular Spaces," *Transactions of the AIChE*, Vol. 38, 1942, p. 593.

[14]Paske, J. M., Papadopoulos, P., George, C. M., France, D. M., and Minkowycz, W. J., "Steady-State Post-Critical Heat Flux Heat Transfer to a Refrigerant," *Journal of Thermophysics and Heat Transfer*, Vol. 6, No. 2, 1992, pp. 314–320.

[15]Dittus, F. W., and Boelter, L. M. K., "University of California, Berkeley, Class Notes," *Publications of Engineering*, Vol. 2, 1930, p. 443.

[16]Gnielinski, V., "New Equations for Heat and Mass Transfer in Turbulent Pipe and Channel Flow," *International Chemical Engineering*, Vol. 16, 1976, pp. 359–368.

[17]Shin, S. K., and France, D. M., "Thermally Developing Flow in an Annulus with a Boiling Boundary," *Journal of Thermophysics and Heat Transfer*, Vol. 2, No. 3, 1988, pp. 235–241.

[18]Lopina, R. F., and Bergles, A. E., "Heat Transfer and Pressure Drop in Tape Generated Swirl Flow of Single-Phase Water," *Journal of Heat Transfer*, Vol. 91, 1969, pp. 434–445.

[19]Baumeister, K. J., Hamill, T. D., and Schoessow, G. J., "A Generalized Correlation of Vaporization Times of Drops in Film Boiling on a Flat Plate," *Proceedings of the 3rd International Heat Transfer Conference*, Vol. IV, AIChE, 1966, pp. 66–73.